acta physica slovaca vol. 55 No. 3, 341 – 350 **June 2005**

INJECTION AND EXTRACTION CURRENTS IN THIN ZIRCONIUM OXIDE FILMS[1]

H. Frank[2]
Department of Solid State Engineering, Faculty of Nuclear Sciences and Physical Engineering
Czech Technical University, Trojanova 13, 120 00 Prague 2, Czech Republic

Received 11 February 2005, accepted 23 March 2005

The conductivity mechanism of zirconium oxide films grown 1554 days in water of 360°C on tubes of Zr1Nb, Zr Sn Nb(Fe), and IMPZry-4, respectively, was investigated by I-V measurements at various temperatures. The high current flowing at voltage application is due to electron injection and decreases slowly obeying a power law until steady state conditions by a built-up space charge are reached. Switching off the voltage, a short-circuit current of opposite polarity due to the outflowing space charge is observed, which decreases obeying a power law. By integration of the extraction current, the space charge as linear function of the injection voltage could be assessed, the extracted charge being equal to the injected charge.

PACS: 73.40.Rw, 73.50.Gv, 73.61.Ng

1 Introduction

The results presented in this paper were achieved by continuing the investigation of the transport properties of oxide layers of zirconium alloys described earlier [1]. Zirconium alloys are being used in nuclear light water reactors as fuel cladding and channel box materials because of their enhanced corrosion resistance [2,3]. In a high-temperature aqueous environment, oxides are formed by diffusion of oxygen ions through the built-up layer, combining with zirconium ionized by electron emission [4]. The corrosion of the zirconium is due to oxide formation by the transfer of electrons from the metal to water, whereby oxygen ions flow in the opposite direction.Thus the corrosion rate depends largely on the electron motion, which is governed by the electrical conductivity of the oxide layer. The investigation of the electrical properties of the oxide is therefore of interest for understanding the mechanism of oxide forming and corrosion resistance. Howlader et al. [4] concluded that electron conduction dominates the electrical conductivity of Zircaloy oxide films. It is well known [4, 5, 6] that ZrO_2 is predominantly an electronic high-resistivity semicoductor with a low amount of ionic conduction. The band gap is approximately 5 eV, the work function 4.0 eV and the relative permittivity 22.

[1] Presented at SSSI-IV (Solid State Surfaces and Interfaces IV) Conference, Smolenice, Slovakia, 8–11 Nov. 2004.
[2] E-mail address: frank@km1.fjfi.cvut.cz

2 Experimental

Oxide films on tubes 30 mm long and of 9 mm outer diameter from the zirconium alloys Zr1Nb, Zr Sn Nb(Fe) and IMPZry-4 had been grown at VVER conditions in water of 360°C for 1554 days [7]. Gold electrodes 200 nm thick were vacuum evaporated onto the specimens wrapped in Al-foil with circular openings 6.0 mm in diameter. Owing to the large contact area of 0.283 cm^2 guard rings appeared to be unnecessay, no difference was found with readings taken with and without guard rings. The specimens were mounted in a small thermostat with a maximum temperature of 220°C. The abraded front ends of the tubes of shining zirconium metal were in direct contact with pressed-on copper electrodes, on which a thermocouple was mounted for temperature control. The current was measured with a two-electrode arrangement, using only one contact to each electrode. The contact resistance between the copper electrodes pressed onto the metallic bulk zirconium is certainly to be neglected, the same being true for the resistance between the gold electrode and the pressed-on 0.3 mm thick phosphorbronze contact spring. A stabilized voltage source could be connected with the positive terminal to the zirconium metal contact, while the negative terminal was earthed to the pico-amperemeter common. The input terminal was connected via the contact spring to the gold electrode. The voltage drop of the pico-amperemeter was limited to 10 mV max. and could be neglected for source voltages larger than 2V.

3 Results

Measurements were taken at constant temperatures, i.e., at room temperature and then at about 60, 80, 100, and 120°C, respectively. The electric current measurement was very time consuming. The current on the application of voltage was much higher (up to over tenfold) than at equilibrium, which was reached only after a long time (up to several hours)

A typical case is shown in Fig. 1. After about 30 min. the drop ended and the current remained constant. This value can be used for further computation of transport parameters. When the voltage was switched off, an extraction current of opposite sign could be observed (curve b in Fig. 1), which had the same time dependence as the aforeflowing injection current. The time dependence of the difference of the total current and of the steady current is plotted in curve c in Fig. 1, which proves to be the same as the extraction current. The system behaves like a storage cell. The charge which had been built up by the flowing injection current has remained unchanged due to the high resistivity of the oxide layer and is the source of the extraction current when the sample is shorted by the pico-amperemeter.

When the data of Fig. 1 are plotted in a logarithmic scale, as shown in Fig. 2, then the straight line put through the measuring points of the extraction current indicates a power law of the type.

$$I = Bt^{-n}, \tag{1}$$

where I is the current, the constant B is the current at $t = 0$ and $n < 1$ is the exponent. Due to the additional constant current part at injection, the power law of the pure injection current does not appear as a straight line in the upper part of Fig. 2.

The time dependence of injection and extraction currents at various injection voltages is depicted in Fig. 3a, and Fig. 3b, respectively. The different inclination of the fitted power law

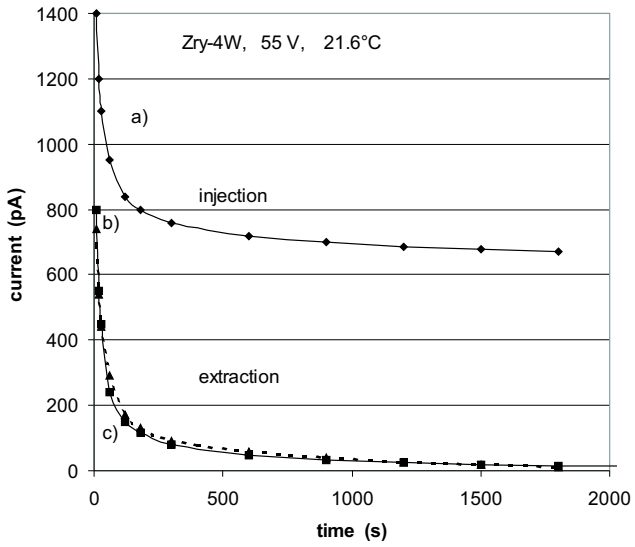

Fig. 1. IMPZry-4, room temperature, Time dependence of current. a) After application of 55 V, the injection current is slowly diminishing and steady space- charge limited current is reached after 2000 s. b) Voltage source switched off, sample short-circuited via pico-amperemeter. Extraction current (of opposite sign) slowly diminishing. c) Pure injection current, values of a) subtracted by the value of the steady space-charge limited current, showing that injection and extraction are equal.

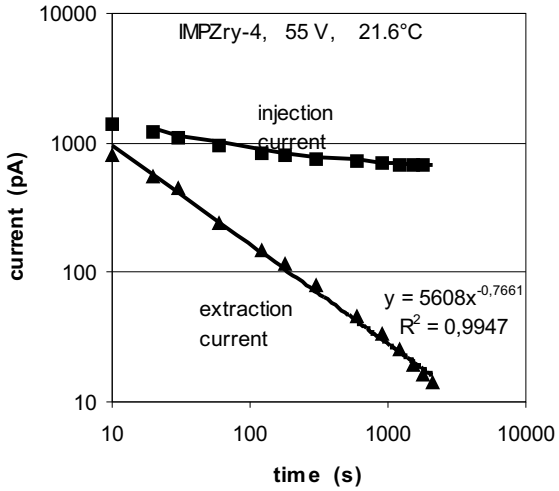

Fig. 2. Values of Fig. 1 in a logarithmic scale.

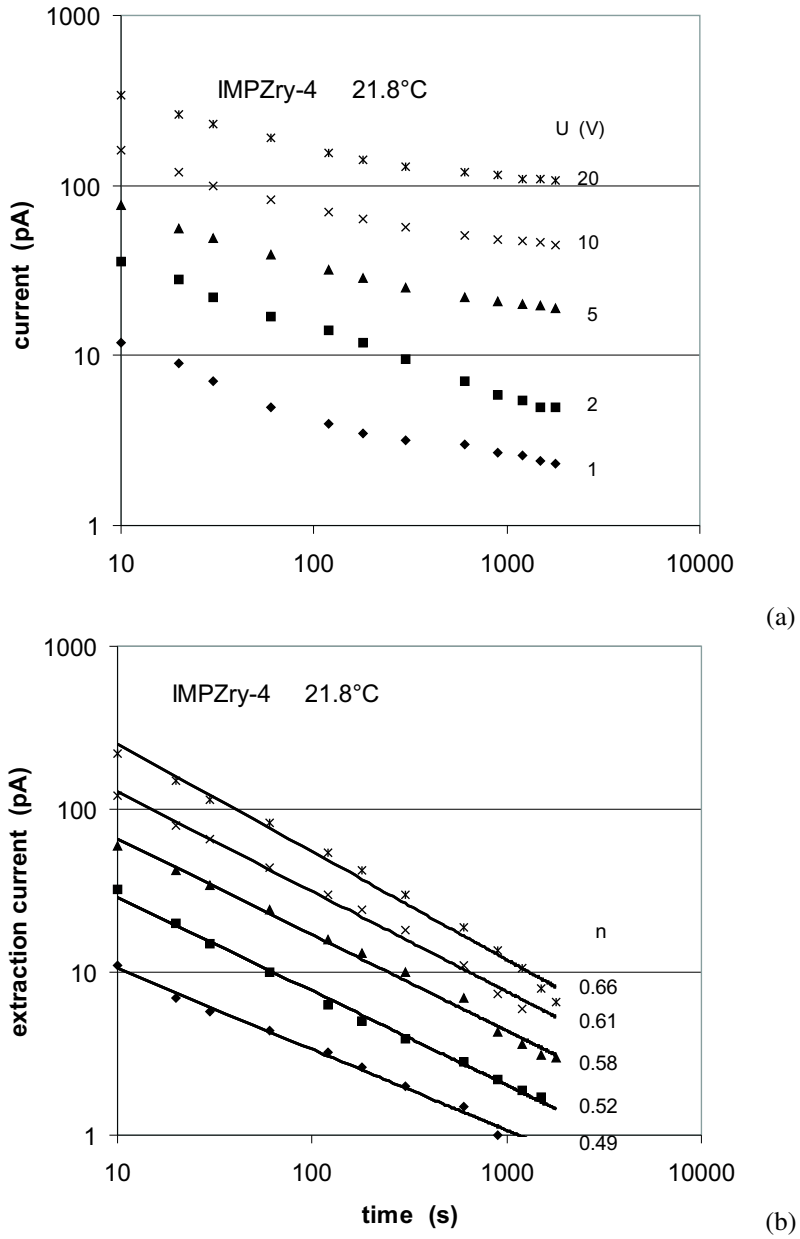

Fig. 3. (a) Time dependence of injection currents with different applied voltages. The power law of the the dropping injection current is not apparent as a straight line, due to the additional part of the steady current, which is asymptotically reached after the end of the injection. (b) Time dependence of the extraction currents (of opposite polarity, not shown in the logarithmic scale). Straight lines of the computed regression prove the power law of eq. (1).

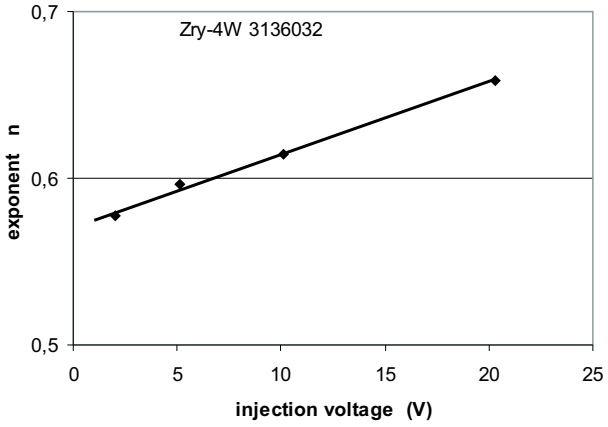

Fig. 4. Linear dependence of the exponent on the injection voltage, values taken from Fig. 3b. The value of n, measured at 1 V, has been excluded, as conditions for space charge limited current had not yet been reached.

lines shows that the value of the exponent n depends on the injection voltage.With IMPZry-4 it is increasing, as shown in Fig. 4, with the values taken from Fig. 3b, but on the other two samples it was decreasing. The values of the steady state current, taken from Fig. 3b, wich had been reached after the proper time needed to complete the injection phase, are plotted in Fig. 5 for the applied injection voltages, creating the I-V characteristics .

In Figs. 1–3, it is apparent that the current at injection is larger than the short-circuit current at extraction by the value of the steady-state current. This implies that the total current flowing at voltage application is composed of a constant equilibrium part, and a time dependent injection current, building up the space charge. Therefore, meaningful current readings for conductivity determination cannot be taken until the space-charge forming process has been completed and steady-state conditions for the space-charge limited current have been reached.

The I-V characteristis are non-linear and, limited to lower voltages, the asymetry of the characteristics can be neglected. Then the positive branch of the characteristics, as shown in Fig. 5, can be approximated by a second-order polynomial

$$I = aU^2 + bU + c, \tag{2}$$

where c is the short-circuit current flowing without external voltage, being generated by the existence of an inner voltage U_0, either by the remaining space charge, or by continuing oxidation at higher temperatures. The linear term describes the current obeying Ohm's law, and $b = 1/R$ defines the resistance $R = w\rho/A$ of the sample with thickness w, contact area A, and resistivity ρ. The quadratic term expresses the curvature of the characteristics and, as has been shown in [1], is due neither to Schottky emission nor to the Poole-Frenkel mechanism, but is the consequence of an existing space-charge limited current according to the Mott-Guerney relation [8]

$$J = 9\varepsilon\varepsilon_0\mu V^2/(8w^3), \tag{3}$$

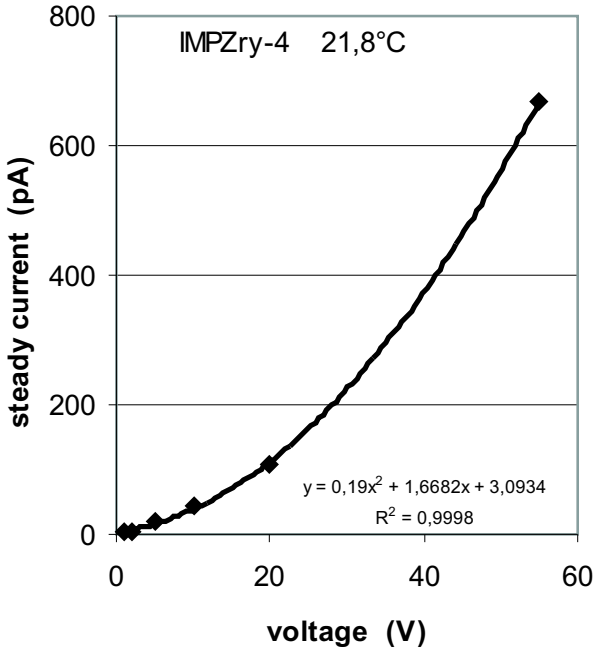

Fig. 5. I-V characteristics proving eq. (2). Steady state current values taken from Fig. 3a.

where *J* is the current density, ε and ε_0 are the relative and vacuum permittivity, respectively, and μ is the mobility of the current carriers. Using the coefficient a of eq. (2) and eq. (3), mobility and carrier concentration can be computed

$$\mu = 8aw^3/9A\varepsilon\varepsilon_0, \tag{4}$$

$$\rho = 10^{12}A/bw, \tag{5}$$

when the current is given in pA

$$N = 1/e\mu\rho. \tag{6}$$

At temperatures above 60°C, the short-circuit current I_0 can be reduced to zero by an adequate compensation voltage, which has the opposite polarity of the zero voltage U_0. This means that the I-V-characteristics do not pass through the origin, and the power needed for the short-circuit current flow is supplied by thermal energy, liberating either the rest of the space charge or activating the continuing oxidation. Using the linear part of the characteristics at the origin, $U_0/I_0 = R$ can be used to calculate the resistivity at higher temperatures. This has the advantage of short measuring times because no external voltage and no waiting for the end of injection is necessary.

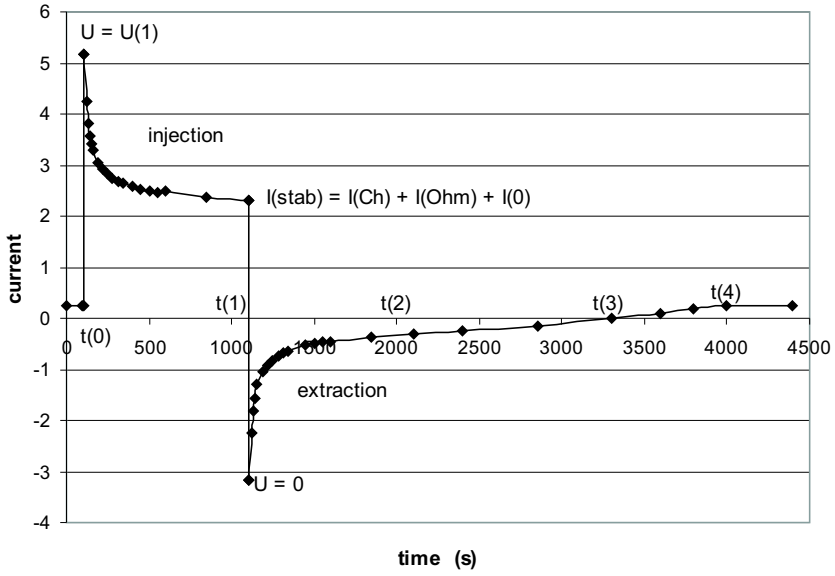

Fig. 6. Time behaviour of injection and extraction currents (schematically, after typical measuring results); a) at $t(0)$, voltage $U = U(1)$ is switched on, starting injection, with current decreasing, b) at $t(1)$, voltage switched off, $U = 0$, extraction current $-I = Bt^{-n}$, c) at $t(2)$, end of extraction, zero current $I(0)$ gradually decreasing (may take up to several days), d) at $t(3)$, the decreasing zero current changes sign and reaches at t(4) a constant positive value (can be observed at higher temperatures).

4 Discussion

The existence of space charges accumulated by long-time injection currents was proved by measuring the short-circuit extraction currents, flowing after completed injection, as shown in Figs. 1–3. The time behaviour of the injection and extraction currents is schematically depicted in Fig. 6. Before switching on the measuring voltage, there flows a small zero current, especially at higher temperatures. Activating the voltage $U = U(1)$ at time $t(0)$, starts the current flow, which consists of a time-dependent injection current according to eq. (1), and a time-independent space-charge limited current. This current is the sum of the zero current I_0, expressed as the factor c in eq. (2), the Ohmic part expressed by the linear term in eq. (2), and the space-charge limited part defined by the quadratic term of eq. (2). At time $t(1)$, and with the voltage $U = 0$, the extraction current, of opposite sign to the injection current, flows obeying eq. (1), and after time $t(2)$ remains at the constant value of the zero current. After a time of several hours, up to several days, this current of negative polarity, at first constant and then decreasing, passes through zero at $t(3)$ and changes, at constant temperature, to a positive time- independent current at $t(4)$. The positive current rises exponentially with temperature, as can be seen in Fig. 7.

The extraction current can be expressed by means of eq. (1), and factor B, and exponent n can be obtained by the regression function of the measuring points (inset in Fig. 2).

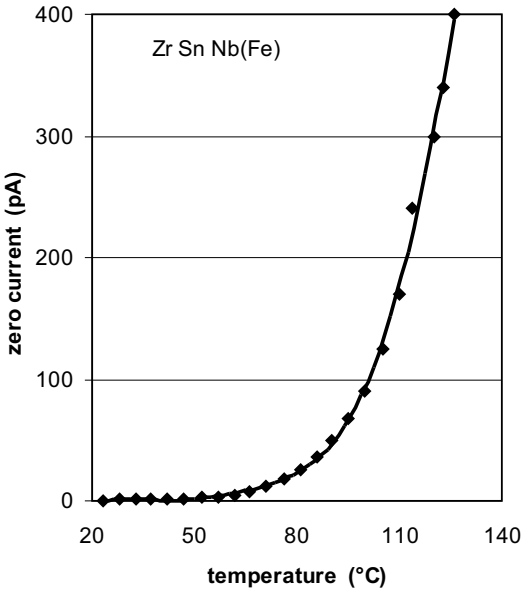

Fig. 7. Temperature dependence of positive zero current produced by continuing oxidation.

The extracted charge Q can be computed by integration

$$Q = \int_{t_1}^{t_2} Bt^{-n}dt = B[t_2^{-n+1} - t_1^{-n+1}]/(-n+1). \tag{7}$$

The extracted charge, computed by means of eqs. (1) and (7) from measuring points in Fig. 3b, is plotted in Fig. 8 as function of the injection voltage. The slope of the straight line in Fig. 8 gives the increase of the extracted charge per unit of injection voltage and is for this sample $dQ/dU = C = 2 \times 10^{-9}$ As/V or 2 nF. Thus the oxide layer behaves like a capacitor with capacity C, or a storage cell, which can be charged and discharged. The mean charge density per voltage and volume unit, (for this sample) is $C/V = 1.68$ μF/cm^3 or , expressed in electron density, 1.24×10^{13} e/V cm^3. The measuring results for all three samples at room teperature are presented in Tab. 1.

Measurements taken at elevated temperatures up to 120°C have been carried out, but are not included in this paper. Although all three samples had been oxidized at the same conditions, there are large differences in electrical parameters. The resistivity rises by a factor of ten, going from Zr1Nb over Zr Sn Nb(Fe) to IMPZry-4. In the same order the injected charge decreases, i.e., the charge is proportional to the conductivity

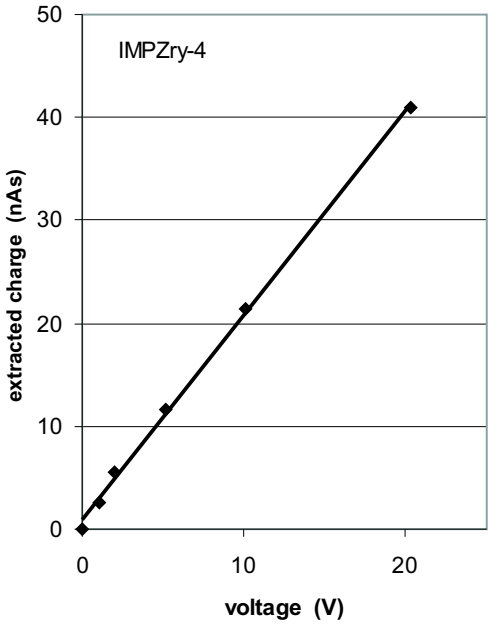

Fig. 8. Extracted charge computed using eq. (7) with values taken from Fig. 3b.

5 Conclusions

It has been demonstrated that the electric current diminuition at the application of potential to the electrodes on the oxide layers of the zirconium alloy samples is due to injection currents building

Tab. 1. Comparison of properties of three Zr alloys.

Parameter/Samples		**Zr1Nb**	**Zr Sn Nb(Fe)**	**IMPZry-4**
Thickness	w (μm)	27.31	35.29	37.55
Geom.factor	A/w (cm)	103.6	80.2	75.4
Rel.permittivity	ε_r –	24	28	18
Loss angle	tanδ –	0.3	0.3	0.05
Resistivity	ρ(Ωm)	4.3x10^{11}	1.3x10^{12}	4.5x10^{13}
Mobility	μ (cm^2/Vs)	1.5x10^{-7}	1.1x10^{-9}	2.0x10^{-8}
Concentration	N (cm^{-3})	1.0x10^{14}	4.4x10^{13}	7.0x10^{12}
Capacity	C (nF)	59	15.1	2
Volume	V (cm$^{3)}$	7.37x10^{-4}	1.0x10^{-3}	1.06x10^{-3}
Density	C/V (μF/cm^3)	76.3	15.1	1.86
Electrons	e/V (e/cm^{3}V)	48x10^{13}	9.4x10^{13}	1.24x10^{13}

up a space charge which can be extracted again as short-circuit current with a hyperbolic time decrease. The space charge is a linear function of the applied voltage. As a consequence of the created space charge, the current in the equilibrium state is space-charge limited, obeying Child's law. The total current is composed of a linear, Ohmic part, and of a non-linear part, increasing with the applied voltage squared, and, especially at higher temperatures, of a constant part of short-circuit current rising exponentially with the temperature. The I-V characteristics are therefore non-linear and, due to the short-circuit part , do not pass through the origin. The energy for the short-circuit current is supplied, at first, by thermally activated liberation of captured electrons from earlier current injection, and finally, as positive zero current, from continuing oxidation by diffusing oxygen.

The annoying time lag of the current after voltage application in high resistivity semiconductors has been explained as the time needed for building up the space charge to get steady state conditions for a stable space charge limited current. It has been shown how to assess the power law of the injection current by measuring the time dependence of the extraction current, and how to get the total of the injected charge by its integration, the extraction current being the negative replica of the time dependent current part in the injection phase, thus $Q_{\text{inj}} + Q_{\text{extr}} = 0$.

Acknowledgement: Support of this work by SKODA-UJP, Praha a.s., is highly appreciated. Special thanks are due to Ms. Věra Vrtílková for providing the oxidized specimens with specified layer thickness.

References

[1] H. Frank: *J. Nucl. Mater.* **306** (2002) 85

[2] D.G. Franklin, P.M. Lang, C.M. Eucken. Garde (Eds.): *Proc. 9^{th} Int. Symp. Nucl. Industry*, ASTM, Philadelphia, p.3, ASTM STP 1132

[3] *Corrosion of Zirconium Alloys in Nuclear Power Plants*, IAEA-TECDOC-684, Vienna 1993

[4] M. M. R. Howlader, K. Shiiyama, C. Kinashita, M. Kutsuwada, M. Inagaki: *J. Nucl. Mater* **253** (1998) 149

[5] M. Inagaki, M. Kanno, H. Maki: *ASTM-STP* **1132** (1992) 437

[6] A. Charlesby: *Acta Metall.* **1** (1953) 348

[7] V. Vrtílková: *private communication*

[8] N. F. Mott, R. W. Guerney: *Electronic Processes in Ionic Crystals*, Clarendon, Oxford, 1940.